Experimental measurements of ultra-lean hydrogen ignition delays using a rapid compression machine under internal combustion engine conditions

Nicolas Villenave, Guillaume Dayma, Pierre Brequigny, Fabrice Foucher

Experimental measurement of ultra-lean hydrogen ignition delays using a rapid compression machine under internal combustion engine conditions

Nicolas Villenave[a,*], Guillaume Dayma[b,c], Pierre Brequigny[a] and Fabrice Foucher[a]

[*] Corresponding author. E-mail address: nicolas.villenave@univ-orleans.fr (N. Villenave)

[a] Univ. Orléans, INSA-CVL, PRISME, EA 4229, F45072, Orléans, France

[b] CNRS-ICARE, 1C avenue de la Recherche Scientifique, 45071 Orléans Cedex 2, France

[c] Université d'Orléans, Orléans Cedex 2, France

Abstract

In order to mitigate greenhouse gas and pollutant emissions from the transportation sector, the use of green e-fuels is planned. Hydrogen spark ignition engines (H_2ICEs) are one of the most important technologies for reducing dependence on fossil fuels. However, these combustion engines are prone to some abnormal combustion phenomena, such as knocking, and require further investigation to get a better understanding of hydrogen combustion properties. This study used a rapid compression machine to present experimental ignition delay measurements of ultra-lean hydrogen/air mixtures under internal combustion engine conditions. The fuel-air ratio ranged from 0.2 to 0.5, the compression temperature varied from 900 to 1030 K, and the compression pressure ranged from 20 to 60 bar. A comparison with often-used and up-to-date hydrogen kinetic mechanisms was performed. The experimental results were consistent and showed an overall good agreement with numerical simulations. The impact of $2\ HO_2 \rightleftharpoons 2\ OH + O_2$ addition on recent kinetic mechanisms was also investigated and presented an average decrease of 20% in ignition

delay. Finally, new third-body efficiencies of H_2O were evaluated and showed no impact on prediction. The aim of this approach was to provide new experimental data for kinetic mechanism validation and optimization.

1. Introduction

Weather-related disasters have escalated due to human activities since the industrial age, and a trillion tons of CO_2 emissions since 1990 are largely responsible for the 1.1°C global median temperature increase in the last decade [1, 2]. To limit the predicted 3-4°C increase in global median temperature by 2050, governments aim to reach the Net Zero Emission scenario [3]. The transport sector, which emitted almost 8,220 Mt of CO_2 in 2021, is one of the most emitting sectors that requires deep decarbonization to meet this target [4]. One of the carbon-free pathways is green e-fuels, such as ammonia or hydrogen, which could be produced by renewable energies. The use of these fuels as substitutes for diesel and gasoline is a promising solution for greenhouse gas reduction. The main properties of these fuels are compared with conventional fuels in Table 1.

38

Table 1 – Hydrogen, Ammonia, Gasoline, and Methane properties at 1 bar, 300 K. Data from [5].

Formula	H_2	NH_3	C_8H_{18}	CH_4	CH_3OH
Lower Heating Values [MJ kg^{-1}]	120	18.8	44.3	50	19.9
Volumetric energy density [GJ m^{-3}]	4.7	11.3	33	9.35	15.72
Stoichiometric air-fuel ratio by mass [-]	34.6	6.05	15	17.3	6.46
Auto-ignition temperature at ambient P [K]	860	950	506	859	465
Research Octane Number [-]	>100	>130	95	120	109
Flammability range in air [ϕ]	0.2 - 6	0.65 - 1.55	0.7 - 4	0.7 - 1.4	0.5 – 4.3
Adiabatic flame temperature at ϕ = 1.0 [K]	2380	2075	2275	2225	2228
Laminar burning velocity at ϕ = 1.0 [m s^{-1}]	2.4	0.07	0.58	0.38	0.4

39

40 Table 1 shows that the use of H_2 as a fuel for internal combustion engines (ICEs) offers many advantages but
41 also challenges: the laminar flame speed of hydrogen is high, almost five times faster than that of gasoline at
42 stoichiometry, which can improve engine efficiency. However, high flame speed and low ignition energy may cause
43 backfires. The adiabatic combustion temperature, higher than that of classical fuels, leads to thermal nitric oxides
44 (NOx) formation. In contrast, hydrogen's wide flammability range allows very lean operations in internal combustion
45 engines. Ultra-lean conditions make it possible to reach low to zero NOx emissions while maintaining higher engine
46 efficiency than gasoline-based ICEs [6]. This conclusion was also underlined by Krishnan Unni et al. [7] using a
47 single-cylinder gasoline engine modified to operate with both gasoline and hydrogen. Brake thermal efficiency
48 measurements were conducted for a wide range of engine speeds (1200 – 3600 RPM) and for different ranges of fuel-
49 air ratios: for lean-to-rich gasoline/oxidizer mixtures (ϕ = 0.8 – 1.4) and for lean hydrogen/oxidizer mixtures (ϕ = 0.4
50 – 0.6). It shows that brake thermal efficiency is almost 10 % higher for hydrogen than for gasoline operation.
51 Hydrogen internal combustion engines (H_2ICEs) are hardly a new development. The aim is to reduce local and
52 global emissions of NOx while increasing efficiency compared to diesel or gasoline-based ICEs. Dimitriou et al. [8]
53 presented a review of hydrogen as a compression ignition engine (CIE) fuel, showing that a hydrogen CIE should
54 present no HC, CO, and CO_2 compared to fossil fuel-based engines, while an increase in the ratio of energy in the
55 brake power to the fuel energy is observed. However, it was also highlighted that without any devices such as exhaust
56 gas recirculation to decrease the flame temperature in the combustion chamber, NOx formation increases, particularly

at high loads. Gomes Antunes et al. [9] presented an investigation of hydrogen-fueled homogeneous charge compression ignition engine performance and operation in a single-cylinder modified diesel engine. A brake thermal efficiency of 45% was obtained under ultra-lean conditions with an equivalence ratio of 0.33 and low levels of greenhouse gases and NOx emissions were observed. Das et al. [10] presented an overview of the development of H_2ICEs since 1930 and highlighted various undesirable combustion phenomena linked to the physicochemical properties of hydrogen such as pre-ignition, backfire, and auto-ignition. Even if the auto-ignition temperature of hydrogen is high, the minimum energy required for hydrogen ignition is low. Thus, a small amount of energy deposit from a hot surface or a spark plug could ignite the mixture before the right time. On one hand, pre-ignition occurs when the mixture is in contact with a hot spot in the cylinder and when intake valves are open, thus implying backfiring. On the other hand, auto-ignition occurs, similarly because of a hot spot, but after the intake valves close, creating knock (abnormal combustion). Knocking produces a high heat release transfer to the combustion chamber walls and an overpressure in the cylinder. This phenomenon directly impacts engine performance, emissions, and durability and can even break it. Therefore, it is important to study auto-ignition behavior, especially ignition delay, which is one of the fundamental properties driving the knock process of hydrogen/air mixtures in ICEs condition.

Under lean conditions, the adiabatic flame temperature is much lower than at stoichiometry, so the conditions for autoignition are less favorable. However, fuel stratification in the combustion chamber potentially enhances the autoignition phenomenon under lean conditions. Indeed, Hamzehloo et al. [11] performed Reynolds-Averaged Navier-Stokes calculations to study mixture formation and combustion in a cylinder with direct injection in a hydrogen spark-ignition engine. Both simple and double injections were used, and results showed that the mixture is stratified in the combustion chamber with equivalence ratios varying from $\phi = 0.1$ up to 0.8 at ignition timing. Law et al. [12] calculated the overall activation energy of H_2 flames as a function of the equivalence ratio for $p = 0.6$ to 5 atm. Results showed a significant increase in the overall activation energy in the lean mixture region upon decreasing the equivalence ratio. In addition, a higher pressure leads to a greater slope of the overall activation energy as a function of the equivalence ratio. Thus, in engine-like conditions where the pressure can have a magnitude twenty times higher than in the aforementioned study, the overall activation energy required for the ignition of locally lean mixtures is much higher than for the ignition of locally rich mixtures. This suggests that stratification in global lean hydrogen mixtures may potentially promote pre-ignition and auto-ignition phenomena.

Abnormal combustion is the reason why ignition delay measurement under ICE conditions needs to be investigated since, to the best of the authors' knowledge, the literature on ultra-lean ($\phi \leq 0.4$) hydrogen/air ignition delays, using a rapid compression machine, under ICE conditions is rather limited. These experimental data are required to better understand autoignition and knocking issues. Finally, these data are invaluable targets in order to test H_2 kinetic mechanisms under ICE conditions, mechanisms that can be used in high-fidelity simulations to design and control new propulsion technologies. Several experimental devices are used to measure ignition delay times under different conditions such as motored engines, flow reactors, shock tubes (ST), and rapid compression machines (RCM) [13]. ST and RCM are the most relevant for measuring delays in engine conditions as highlighted in Fig 1.

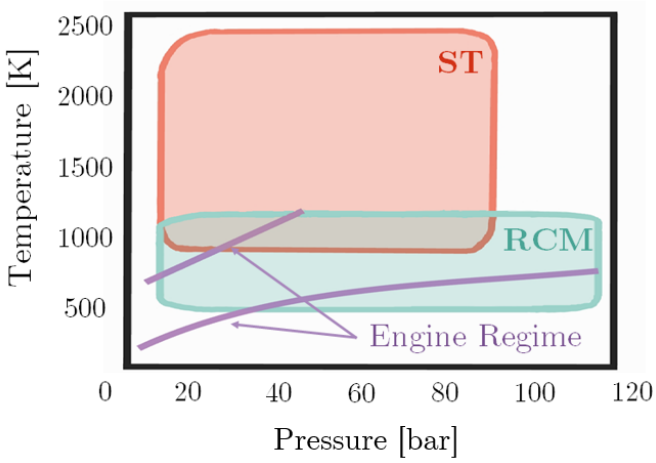

Figure 1 – Temperature-pressure diagram of operation range for Rapid Compression Machine (RCM), Shock Tubes (ST), and internal combustion engines.

Several studies have been conducted on the measurement of hydrogen ignition delays using ST. In the study carried out by Pang et al. [14] the ignition delays of hydrogen/oxygen/argon mixtures were investigated under conditions of T = 908 - 1118 K, p = 3.0 - 3.7 atm, and 4% - 15 mole fraction of H_2. Experimental results were compared to kinetic mechanisms and showed good agreement. Notably, the comparison highlighted the influence of a key reaction, $H + O_2 + M \rightleftharpoons HO_2 + M$, in the low-temperature region. Subsequently, Hu et al. [15] showed that this reaction also predominated at high temperatures by investigating $H_2/O_2/N_2$ mixtures at T = 1000 - 1600 K, p = 1.2 - 1.6 atm, and ϕ = 0.5 - 1.0. In addition, results showed that the global activation energy of hydrogen increases with

pressure. In order to study hydrogen-blended fuels, ignition studies are crucial to know the impact of H_2 on kinetics. For instance, Pan et al. [16] used a high-pressure ST to quantify ignition delay times of stoichiometric $H_2/C_2H_6/O_2/Ar$ mixtures at p = 1.2, 4.0, and 16.0 atm and with hydrogen blends of 70 %, 90 %, 97 %, 100%. At p = 4.0 and 16.0 atm, results pointed out that hydrogen addition decreases ignition delays. At p = 1.2 atm, hydrogen addition decreases ignition delays at high temperatures between 900 K - 1250 K. Finally, at fixed composition, when pressure increases, ignition delays also decrease. Shock tube investigations are essential because they can cover a wide range of temperatures, making possible to study hydrogen ignition behavior at really high temperatures. However, as displayed in Fig. 1, these conditions are not appropriate for current interest in ICEs. RCM is a better-suited device to cover engine-like conditions. There are several studies investigating hydrogen blended with other fuels using a RCM [17 – 20] and showing that hydrogen addition tends to promote mixture reactivity and decreases ignition delays.

However, concerning RCM experiments, there are only a few experimental studies of ignition delays for pure hydrogen/oxidizer lean-to-rich mixtures at low-to-high pressure and temperature. Lee et al. [21] explored $H_2/O_2/Ar$ autoignition above the second explosion limit i.e. p_C = 6 - 40 bar and T_C = 950 - 1050 K. Results showed that energy release is much greater over the second explosion limit in comparison with the first one. Lee et al. also highlighted that the reaction of $HO_2 + H_2 \rightleftharpoons H_2O_2 + H$ appears as one of the most essential reactions for high-pressure conditions because of H radical production. Mittal et al. [22, 23] investigated the autoignition of $H_2/O_2/Ar/N_2$ and $H_2/O_2/CO/Ar/N_2$, at p_C = 15 to 50 bar, T_C = 950 to 1100 K and equivalence ratios from 0.36 - 1.6. For pure hydrogen mixture, at p_C = 15/30/50 bar, T_C = 950-1040 K, and ϕ = 1.0, results showed that for increasing pressure, ignition delays decrease. This trend agrees with the fact that reactions involving the consumption and formation of HO_2 and H_2O_2 become important at high pressure. Moreover, the study compared experimental data with numerical simulations performed using different kinetic mechanisms and found that the mechanism of Ò Conaire et al. [24] agreed better with their experimental data. Das et al. [25] studied the autoignition of dry and moist hydrogen/oxidizer mixtures for p_C = 10, 30, and 70 bar, T_C = 907 K - 1048 K at stoichiometry and with a water addition of 0%, 10%, and 40% vol. In dry stoichiometric $H_2/O_2/N_2$ mixtures, results revealed that ignition delays decrease when the compression pressure increases. Furthermore, for p_C = 30 and 70 bar, ignition delays are shorter with 10% and 40% of water addition. However, at lower pressure, p_C = 10 bar, water injection makes delays longer. A brute force sensitivity analysis was performed. At higher pressure, the chain branching reaction $H_2O_2 + M \rightleftharpoons 2\ OH + M$ was

130 improved because water molecules are good third-body collision partners. Nevertheless, water addition increases the
131 consumption of H radicals by $H + O_2 + H_2O \rightleftharpoons HO_2 + H_2O$, and indirectly, inhibits the production of OH radicals
132 from $H + O_2 \rightleftharpoons O + OH$ and $H + HO_2 \rightleftharpoons 2\ OH$. Moreover, it showed that H_2/O_2 and $H_2/O_2/H_2O$ kinetic mechanisms
133 could present significant discrepancies in numerical simulations compared to experimental results at stoichiometric
134 conditions. Kéromnès et al. [26] performed an experimental and modeling study of hydrogen and syngas oxidation
135 and ignition delay times for $H_2/O_2/N_2/Ar$ highly-dilute (inert/O_2 = 13) stoichiometric mixtures at 70 bar and for lean
136 ($\phi = 0.5$) $H_2/O_2/N_2/Ar$ mixtures at 8, 16 and 32 bar were investigated. According to the author's review, these findings
137 represent the first measurements of ignition delays for lean hydrogen mixtures under engine-relevant conditions
138 within the low-to-intermediate temperature region. Consequently, the literature review showed that further
139 experimental investigations under engine-like conditions and lean mixtures are required to test the validity of the
140 most recent kinetic mechanisms. Indeed, this validation becomes increasingly crucial in the context of spark ignition
141 engines (SIEs), where accurate kinetic mechanisms play a major role in understanding and optimizing processes.
142 Under SIEs conditions, the in-cylinder pressure is crucial to ensure efficient combustion. It can vary from an
143 intermediate-pressure condition, i.e. 30 bar, up to a high-pressure condition, i.e. 120 bar. Therefore, to carry out
144 numerical simulations in ICEs, kinetic mechanisms which do not diverge far from experimental observations with
145 high-pressure variations must be obtained.

146 Besides, Burke et al. [27] analysis reveals that uncertainties in the temperature and pressure dependence of rate
147 constants for HO_2 formation and consumption reactions have a significant impact on the predictive capabilities of the
148 model, especially under high-pressure and low-temperature conditions. These findings highlight the importance of
149 an accurate determination of the relevant rate constants to improve the accuracy and reliability of combustion models
150 in such conditions as SIEs. Therefore, Li et al. [28] kinetic mechanism was updated by paying attention to the
151 pressure-dependence of $H + O_2 + M \rightleftharpoons HO_2 + M$, the temperature-dependence of the $H + HO_2$ branching ratio, and
152 the third-body reaction $O + OH + M \rightleftharpoons HO_2 + M$. However, the contribution of $H + HO_2 \rightleftharpoons H_2O + O$ to combustion
153 modeling was not well understood. This mechanism is still widely used in numerical simulations [29 – 31].
154 Subsequently, Burke et al. [32] turned their attention to the temperature-dependent reaction $OH + HO_2 \rightleftharpoons H_2O + O_2$,
155 which had previously posed challenges in combustion modeling. Finally, in the face of uncertainties from HO_2

consumption and production reaction, Klippenstein et al. [33] very recently suggested some modifications to key reactions. These modifications included the rate constants of 2 $HO_2 \rightleftharpoons H_2O_2 + O_2$ and the addition of 2 $HO_2 \rightleftharpoons 2OH + O_2$ reaction in order to account for H_2O_2 prompt dissociation. This update holds great promise for improving the accuracy of combustion mechanisms in predicting ignition delays and authors will refer to Klippenstein et al. kinetic mechanism, for sake of clarity. Modifications from Burke et al. [27] to Klippenstein et al. kinetic mechanism are reported in Table 2. On the other hand, Konnov et al. [34], Mei et al. [35], and Sun et al. [36] have been recently optimized for hydrogen combustion and are interesting to consider.

Table 2 – Modification from Burke et al. (2012) [27] to Klippenstein et al. (2022) [33] kinetic mechanism.

	A	n	E_a
$HO_2 + OH \rightleftharpoons H_2O + O_2$			
Burke et al. (2012) [27]	2.89E+13	0.00	-4.97E+02
Burke et al. (2013) [32]	1.93E+20	-2.49	5.84E+02
(modification)	Duplicate	Duplicate	Duplicate
	1.21E+09	1.24	-1.31E+03
Klippenstein et al. (2022) [33]	1.93E+20	-2.49	5.84E+02
	Duplicate	Duplicate	Duplicate
	1.21E+09	1.24	-1.31E+03

2 HO_2 ⇌ H_2O_2 + O_2			
Burke et al. (2012)	4.20E+14	0.00	1.20E+04
	Duplicate	Duplicate	Duplicate
	1.30E+11	0.00	-1.63E+03
Burke et al. (2013)	4.20E+14	0.00	1.20E+04
	Duplicate	Duplicate	Duplicate
	1.30E+11	0.00	-1.63E+03
Klippenstein et al. (2022) (modification)	1.93E-02	4.12	-4.96E+03
2 HO_2 ⇌ 2 OH + O_2			
Burke et al. (2012)	-	-	-
Burke et al. (2013)	-	-	-
Klippenstein et al. (2022) (addition)	6.41E+17	-1.54	8.54E+03

Units are cm^3 mol s cal K, $k = A\ T^n\ exp(-E_a/RT)$

As a result, the purpose of this study was to measure ignition delay times of lean and ultra-lean hydrogen/air mixtures within ϕ = 0.2 – 0.5 range, while subjecting them to SIEs conditions, specifically compression pressures (p_C) ranging from 20 to 60 bar and compression temperatures ranging from T_C = 900 – 1030 K. The collected data were then compared with different H_2/O_2 chemical kinetic mechanisms available in the literature in order to assess their validity under ICEs conditions. Finally, a brute force sensitivity analysis will be conducted to compare the two most consistent models and assess the importance of the 2 HO_2 ⇌ 2 OH + O_2 reaction, which is not considered in the other detailed chemical kinetic mechanisms.

2. Experimental Setup

Ignition delay times represent the duration for a mixture to self-ignite under specific thermodynamic conditions and are influenced by the nature of the fuel, the temperature, the pressure, the equivalence ratio, and the dilution. As

already mentioned, the accurate determination of ignition delay times holds significant relevance in the comprehensive investigation of combustion phenomena and the development of reliable chemical mechanisms for internal combustion engines (ICEs). A rapid compression machine (RCM) allows for ignition delay times measurement of a specific mixture in stable and homogeneous conditions, for a wide range of pressure and temperature. This experimental setup is defined by the rapid compression of a mixture, using a single or double piston, followed by a very sharp stop of the compression, thereby resulting hypothetically in steady thermodynamic conditions during the induction period, prior to ignition. To ensure this hypothesis, heat losses must be considered as explained in the following. Nonetheless, RCM is a good way to simulate a single compression stroke of an ICE. The experimental setup used in this study is the single-piston RCM similar to the one used at the Argonne National Laboratory [37] and is illustrated in Fig. 2. The RCM piston is pneumatically driven and hydraulically stopped at the end of compression in order to keep the combustion volume constant. The RCM compresses, until a given compression pressure, a premixed mixture to reach the desired compression temperature, at the top dead center. The main characteristics of the RCM are described in Table 2. The piston was designed with a crevice head to capture vortex roll-up and guarantee the homogeneity of the core gas. Nonetheless, if small vortices were formed near the crevice region, as hydrogen has no negative temperature coefficient region, there would be no effect on the ignition delays [20]. This homogeneity of the core gas allows the use of the adiabatic core hypothesis to calculate the conditions at the top dead center in the cylinder (at the end of the compression when the piston stops). The final temperature T_C, the temperature at the end of the compression, when the pressure is p_C, is deduced from the adiabatic core hypothesis i.e. using the isentropic formula as written in Eq. (1).

$$\int_{T_0}^{T_C} \frac{\gamma}{\gamma - 1} \frac{dT}{T} = \int_{p_0}^{p_c} \frac{dP}{P} \tag{1}$$

where T_0 is the intake temperature, p_0 is the intake pressure, and p_C is the pressure at the end of compression.

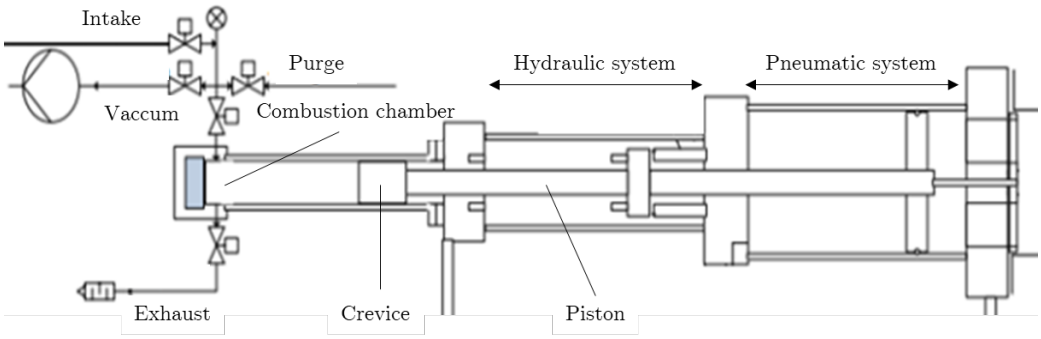

Figure 2 – Rapid compression machine from Orléans University

Table 3 – RCM main characteristics and experimental conditions investigated in this study. The compression ratio corresponds to the volume ratio of the combustion chamber at the bottom dead center configuration and at the top dead center configuration respectively.

Parameters	**Values**
Stroke [mm]	300
Crevice volume [cm^3]	9.94
Compression ratio [-]	13
Piston diameter [mm]	50
Intake temperature T_0 [K]	353 – 393
Intake pressure p_0 [bar]	0.9 – 1.97
Compression temperature T_C [K]	900 – 1030
Compression pressure p_C [bar]	20 – 60

The different reactive and non-reactive mixtures studied here were prepared in a stirred and preheated separate tank prior to the experiment. Non-reactive mixtures were used to assess heat losses by comparing both reactive and non-reactive pressure profiles as displayed in Fig. 3. Furthermore, non-reactive profiles were used as inputs for numerical simulations through the computation of volume time histories. In this case, nitrogen replaced oxygen to

keep the same thermodynamic characteristics as in the reactive case. Exact compositions are provided in Table 3. Prior to filling the premixed tank between each condition, potential residual gases were eliminated by flushing with N_2 and pumping. To control gaseous mass flow rates, Bronkhorst CoriFlow™ flow meters with an accuracy of ± 1% were used with high-purity gases (H_2 99.99%, O_2 99.99%, and N_2 99.99%). The initial temperature of the combustion chamber and preheat temperature of the tank vessel were measured by a K-type thermocouple with an uncertainty of ± 2 K. In-cylinder pressure histories and intake pressures were respectively recorded using an AVL QH32C piezoresistive transducer (± 1%) and a Keller PAA-33X/80,794 (± 1 mbar). For each initial pressure and temperature condition (P_0, T_0), tests were conducted three times to ensure the repeatability of the experiment. The determination of experimental uncertainties is crucial to ensure accurate ignition delays. The statistical error calculation for ignition delays follows the Moffat methodology [38], while the uncertainties in compression temperature were computed using the approach outlined in Baigmohammadi et al. modeling study [39].

Table 4 – $H_2/O_2/N_2$ and H_2/N_2 mixtures for the experiments. Introduced in a 4.18 L tank vessel preheated at 333 K.

Reactive				Non-reactive		
ϕ	H_2 [mole %]	O_2 [mole %]	N_2 [mole %]	H_2 [mole %]	O_2 [mole %]	N_2 [mole %]
0.2	7.75	19.37	72.88	7.75	0	92.25
0.3	11.19	18.65	70.16	11.19	0	88.81
0.4	14.38	17.98	67.64	14.38	0	85.62
0.5	17.36	17.36	65.28	17.36	0	82.64

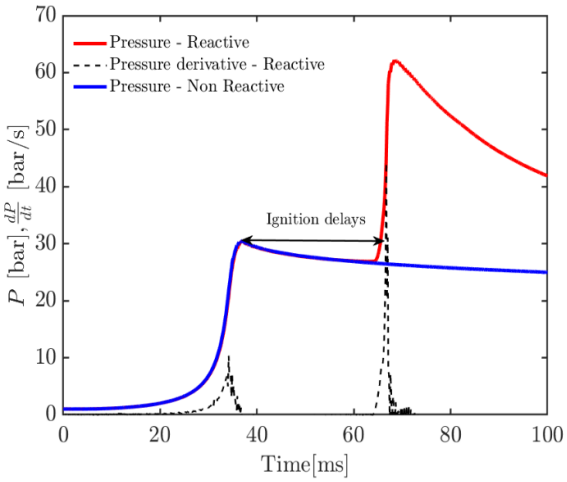

Figure 3 – Experimental pressure profiles from the reactive and the non-reactive case (solid lines). First-order derivative pressure from the reactive case (dash-dotted line). Definition of ignition delays. The reactive case was performed with an $H_2/O_2/N_2$ mixture at $\phi = 0.4$, $T_C = 950$ K, and $p_C = 30$ bar.

3. Numerical simulations

Numerical simulations were carried out using ANSYS CHEMKIN PRO 2020 R1 [39] to validate kinetic mechanisms for ignition delays database of ultra-lean H_2/air mixtures at low-to-intermediate temperatures and low-to-high pressures. The closed-homogeneous reactor model was employed considering a constrained volume and solving the energy equation. This mathematical model assumes that the chemical reaction proceeds in a closed combustion chamber, where the temperature, pressure, and composition are assumed to be spatially uniform. The aim of this model is to describe the progress of the reaction as a function of time. The temperature and pressure imposed are the intake temperature and pressure corresponding to the reactive case. To simulate isentropic compression accurately and consider heat losses, adiabatic core volumes are integrated using the non-reactive pressure trace of each experimental condition studied. Numerical simulations were performed with different hydrogen kinetic mechanisms from the literature. The kinetic model of Burke et al. [32], updated according to Klippenstein et al. study [33], was used. Konnov et al. [34], Mei et al. [35], and Sun et al. [36] were also used. It is worth noticing that Mei et al. kinetic model is an NH_3/H_2 mechanism where H_2 and NH_3 chemical systems were extracted from Hashemi et al. [41] and Shrestha et al. [42] study respectively.

4. Results and discussion

Ignition delay times for lean and ultra-lean (ϕ = 0.2 – 0.5) $H_2/O_2/N_2$ mixtures were measured using a rapid compression machine under internal combustion engines conditions i.e. for intermediate-to-high pressures p_C = 20 – 60 bar and low-to-intermediate temperatures T_C = 900 – 1030 K. Each RCM is unique and it is possible that there are undefined systematic uncertainties. It is therefore interesting to compare ignition delay measurements with results extracted from the literature. As mentioned in the introduction, ignition delay data for lean and ultra-lean hydrogen mixtures under engine-relevant conditions are very limited. Fig 4. gives a comparison between the measured ignition delay times at ϕ = 0.5, p_C = 30 bar diluted with nitrogen, and similar results with nitrogen and argon mix dilution. Results from this study have low dispersion and are in good agreement with those from Kéromnès et al. [26] obtained in a different RCM.

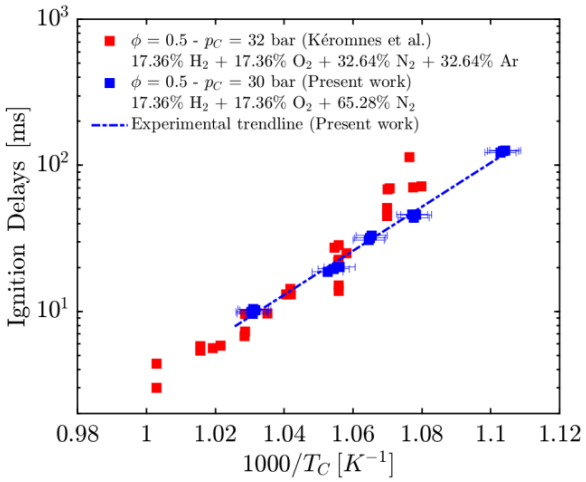

Figure 4 – Ignition delay times comparison with [26] at ϕ = 0.5 and for a fixed compression pressure p_C = 30 bar.

Fig. 5 (a) shows the ignition delay evolution of different lean and ultra-lean $H_2/O_2/N_2$ mixtures (ϕ = 0.2, 0.3, 0.4, and 0.5) at fixed compression pressure (p_C = 30 bar). Ignition delays decrease when ϕ increases as a higher volumetric composition of H_2 leads to a greater production of O, H, and OH radicals, thus promoting reactivity. Fig. 5 (b) displays the ignition delay evolution of ultra-lean $H_2/O_2/N_2$ mixtures, ϕ = 0.4, at different compression pressures (p_C = 20, 30, 40, 50, and 60 bar). Ignition delays decrease when p_C increases as higher molecular collision frequencies between the different species result in reactivity enhancement. Noteworthily, measured ignition delays seem to not suffer from

odd ignitions as they present low dispersion. As a matter of fact, it is due to well-controlled experimental apparatus. First, H_2, O_2, and N_2 are premixed in a separated tank vessel, ensuring a stable and homogeneous mixture. Second, the time gap between combustion chamber filling and compression is short, allowing less time for the mixture to develop spatial homogeneities. Finally, the control of the different RCM variables such as initial temperature and initial pressure enables accurate and repeatable experiments.

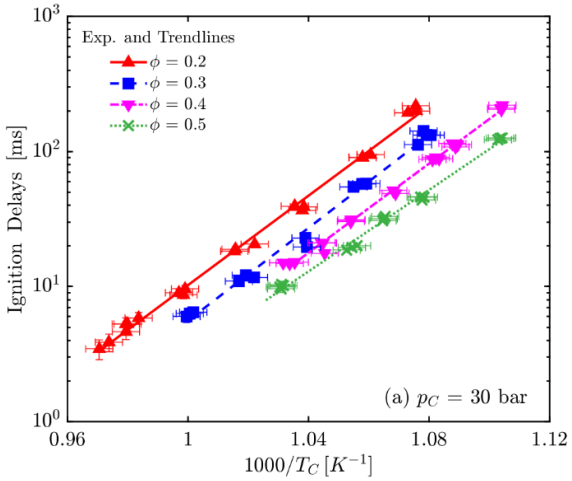

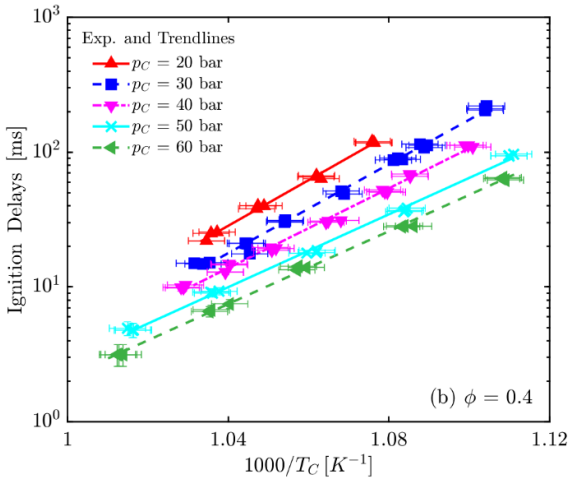

Figure 5 – (a) $H_2/O_2/N_2$ ignition delay times for different equivalence ratios, ϕ = 0.2, 0.3, 0.4, 0.5, and for a fixed compression pressure, p_C = 30 bar. (b) $H_2/O_2/N_2$ ignition delay times for different compression pressures, p_C = 20,

30, 40, 50, and 60 bar, and for a fixed equivalence ratio, $\phi = 0.4$. Symbols: experimental results. Lines: experimental trendlines to guide the eyes.

These new experimental results also give new light on the most recent kinetic mechanisms developed to model H_2/air combustion. Similarly to the experimental method, numerical ignition delays were evaluated with calculated pressure traces obtained from numerical simulations. Fig. 6 presents experimental versus predicted ignition delay times for lean and ultra-lean $H_2/O_2/N_2$ mixtures, (a) $\phi = 0.2$ and (b) $\phi = 0.5$ at a fixed, intermediate compression pressure $p_C = 30$ bar. Results for $\phi = 0.3$ and $\phi = 0.4$ are displayed in the Supplementary Materials. Despite slight discrepancies, numerical predictions display a reasonable overall agreement with experimental results. However, accurate predictions are crucial as slight differences in ignition delays evaluation could have significant impacts on a real spark ignition engine. Mean relative errors between models and experiments were calculated. Recent kinetic mechanisms proposed by Konnov et al. and Sun et al. underestimate ignition delay times, especially at low temperatures, with a mean relative error of 20% and 30% respectively while Mei et al. chemical mechanism is in very good agreement with the present experimental results. Burke et al. model [27] overpredicts the ignition delay times by more than a factor of two in magnitude. Klippenstein et al. model resulted in excellent agreement with our experimental results, especially at higher temperatures, with a mean relative error below 10%. Finally, for $\phi = 0.5$, the trends are reversed and Klippenstein et al. tend to give longer ignition delays while Mei et al. and Sun et al. are in fair agreement. We also evaluated the predictive performance of kinetic mechanisms proposed by Ò Conaire et al. [24], Kéromnès et al. [26], and San Diego [43] kinetic, and have reported the corresponding predicted ignition delays in the supplementary materials.

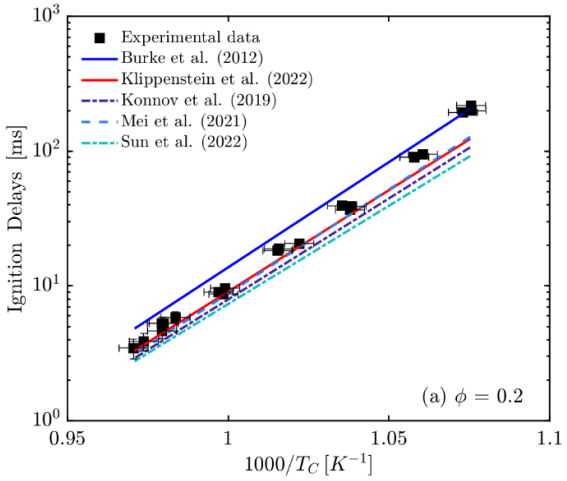

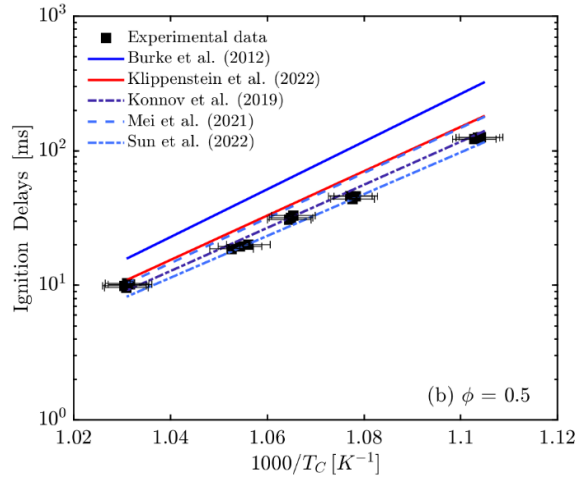

Figure 6 – Comparison of $H_2/O_2/N_2$ ignition delays at $p_C = 30$ bar and for different equivalence ratios, $\phi = 0.2$ (a), 0.5 (b) with numerical predictions. Symbols: Experimental results. Lines: simulations.

The following investigation compares the simulated ignition delay times obtained from different chemical kinetic mechanisms with experimental ignition delays for ultra-lean H_2/air mixtures at a fixed equivalence ratio $\phi = 0.4$, under medium-to-high pressures, i.e. $p_C = 20 – 60$ bar, and for low-to-intermediate compression temperatures, i.e. $T_C = 900 – 1030$ K. Fig. 7 presents the evolution of ignition delay times as a function of the reciprocal temperature, for $p_C =$ (a) 30, (b) 60 bar and for $\phi = 0.4$. Results at $p_C = 20$, 40, and 50 bar are displayed in the supplementary materials. Generally, results obtained from the different kinetic mechanisms are in good agreement with the experimental data, except for Burke et al. model [27].

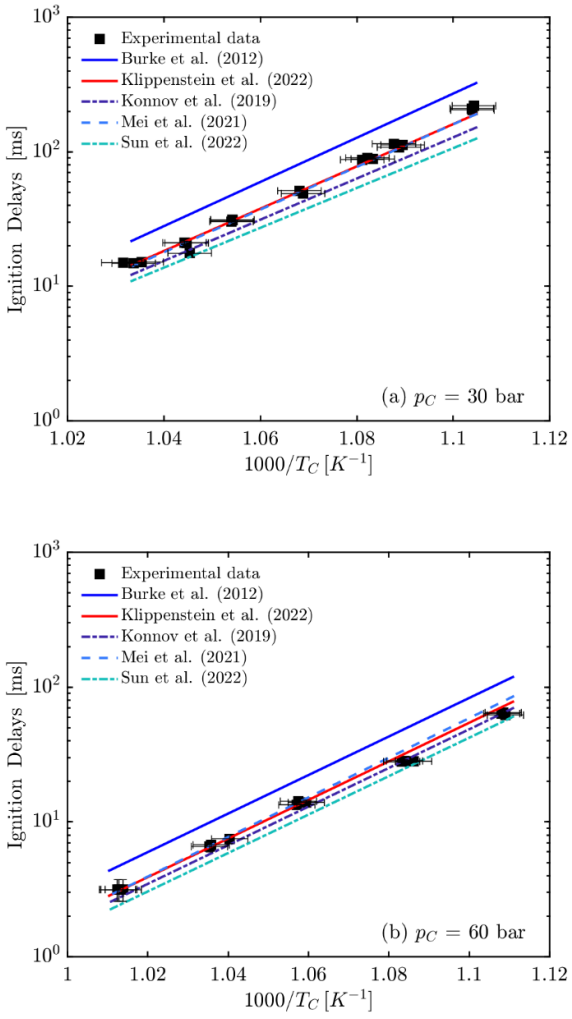

Figure 7 – Comparison of $H_2/O_2/N_2$ ignition delays at ϕ = 0.4 and for different compression pressures, p_C = 20 bar, (a), p_C = 60 bar (b). Symbols: Experimental results. Lines: simulations.

In terms of predictions of ignition delays, it was observed that Klippenstein et al. and Mei et al. kinetic mechanisms demonstrate excellent agreement with the experimental results as the pressure increases, especially at high temperatures. However, Konnov et al. and Sun et al. kinetic mechanisms are in better agreement with the experimental data at higher pressures only in the lowest temperature region. At p_C = 20 bar, Klippenstein et al. model overpredict slightly ignition delays while Mei et al. remains in good agreement at high temperatures as well as Konnov et al. and Sun et al. models. Since Burke et al. [27] kinetic mechanism is often used in ICEs direct numerical

simulations [29 – 31], it is relevant to compare the deviation of the initial model with the Klippenstein updates with the recently published 2 $HO_2 \rightleftharpoons$ 2 OH + O_2 reaction [33]. Fig. 8 (a) shows the relative difference with respect to the initial mechanism by varying the equivalence ratio at fixed compression pressure. As can be seen, the difference between the original and updated versions is rather constant with the equivalence ratio and the temperature under the investigated experimental conditions.

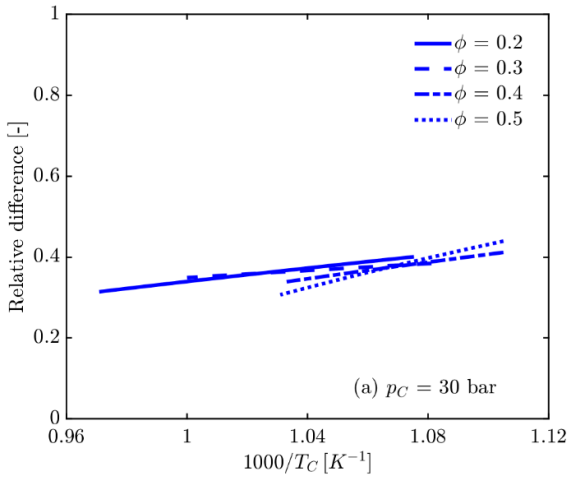

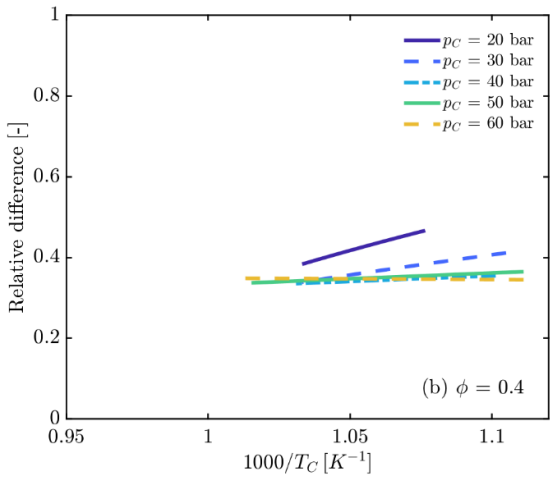

Figure 8 – Relative difference of ignition delays predicted by Burke et al. and by the updated Burke et al. kinetic mechanisms with the addition of 2 HO_2 = 2 OH + O_2 (R16) reaction. (a) p_C = 30 bar and varying the equivalence ratio. (b) ϕ = 0.4 and varying the compression pressure.

The 2 $HO_2 \rightleftharpoons$ 2 OH + O_2 reaction (R16) has a strong promoting effect on the overall reactivity of Burke et al. [27] mechanism leading to a reduction in ignition delays by 30%. This additional reaction also promotes the reactivity of the other three mechanisms: ignition delay times calculated with Mei et al. including (R16) are for instance shortened by 15-21% at ϕ = 0.4 and p_C = 20 bar (see Supplementary Material). Therefore, ignition delay times calculated with Mei et al. being already in good agreement with our measurements, are now underpredicted with (R16) included. Noteworthily, Konnov et al. and Sun et al. were both predicting faster ignition than experimentally observed and are now significantly underpredicting ignition delay times under these ultra-lean, high-pressure, and intermediate temperature conditions. To conduct a comprehensive analysis of the impact of the reaction (R16), a brute force sensitivity analysis was performed on H_2/O_2 reactions using the kinetic mechanisms proposed by Mei et al. and Klippenstein et al. study. The sensitivity coefficient S_i for i-th reaction is calculated as : $S_i = (\tau_{2k_i} - \tau_{(1/2)k_i}/\tau_{k_i})$ where $\tau_{\alpha k_i}$ is the ignition delay calculated by multiplying the Arrhenius factor of the rate constant k_i by a factor α (here a = 1/2, 1 or 2). Only reactions exhibiting sensitivity to constant rate modifications are presented in Table 5 shown in Fig. 9. As can be seen, reactions (R1), (R3), (R11), (R18), and (R20) have the same rate constants, giving similar sensitivity coefficients and traducing similar effects on reactivity enhancement. However, regarding reaction (R17), the sensitivity coefficient is 30% higher in Klippenstein et al. compared to Mei et al. Consequently, (R17) inhibits the ignition in Klippenstein et al. more than in Mei et al. Alongside, the introduction of (R16) in Klippenstein et al., absent in Mei et al., helps counterbalance the decreased reactivity caused by (R17). Notably, the sensitivity coefficient of (R16) in Klippenstein et al. is approximately $S_{(R16,K)}$ = -0.30, indicating a tendency to enhance reactivity. Thereby, it is clear that (R16) has an overall promoting effect in H_2/O_2 kinetic.

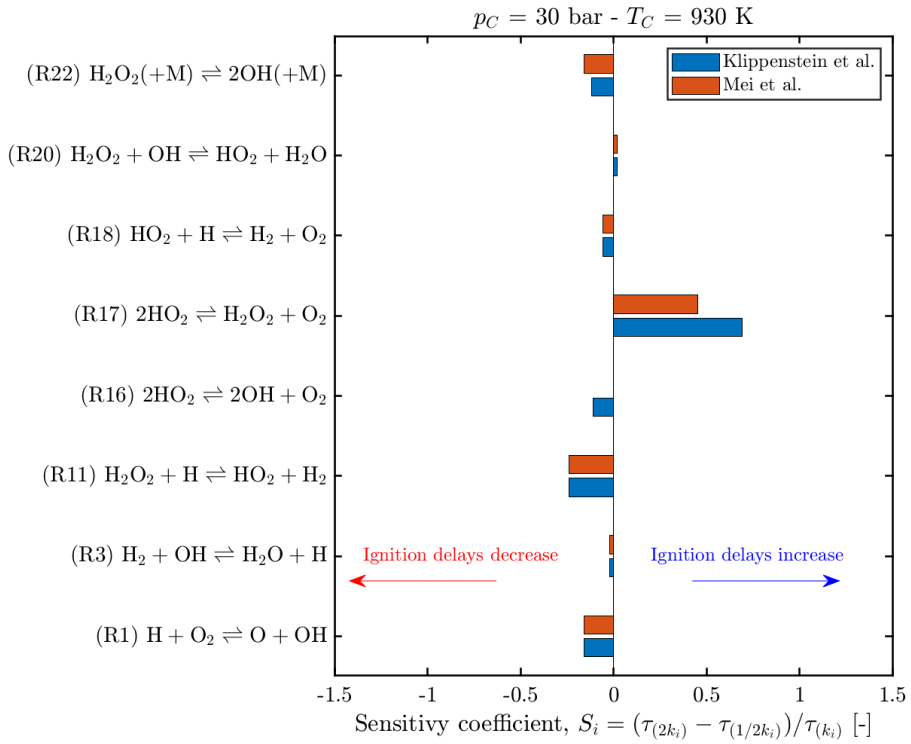

362

363 Figure 9 – Brute force sensitivity analysis on ignition delays for H_2/O_2 reactions for Klippenstein et al. and Mei et al.

364 kinetic mechanisms at p_C = 30 bar and T_C = 930 K.

Table 5 – Differences between Klippenstein et al. [33] and Mei et al. [35] kinetic mechanisms.

	A	n	E_a
(R22) H_2O_2 (+M) ⇌ 2 OH (+M)			
Klippenstein et al. [33]	2.0E+12	0.9	4.8749E+04
Mei et al. [35]	=	=	=
(R20) H_2O_2 + OH ⇌ HO_2 + H_2O			
Klippenstein et al.	1.74E+12 Duplicate 7.59E+13	0.0 Duplicate 0.0	3.18E+02 Duplicate 7.27E+03
Mei et al.	=	=	=
(R18) HO_2 + H ⇌ H_2 + O_2			

Klippenstein et al.	2.75E+06	2.09	-1.451E+03
Mei et al.	=	=	=
(R17) $2\ HO_2 \rightleftharpoons H_2O_2 + O_2$			
Klippenstein et al.	1.93E-02	4.12	-4.96E+03
Mei et al.	1.179E+09 Duplicate 1.251E+12	0.771 Duplicate 0.295	-1.825E+03 Duplicate 7.397E+03
(R16) $2\ HO_2 \rightleftharpoons 2\ OH + O_2$			
Klippenstein et al.	6.41E+17	-1.54	8.54E+03
Mei et al.	Not considered		
(R11) $H_2O_2 + H \rightleftharpoons HO_2 + H_2$			
Klippenstein et al.	4.82E+13	0.0	7.95E+03
Mei et al.	=	=	=
(R3) $H_2 + OH \rightleftharpoons H_2O + H$			
Klippenstein et al.	2.16E+08	1.51	3.43E+03
Mei et al.	=	=	=
(R1) $H + O_2 \rightleftharpoons O + OH$			
Klippenstein et al.	1.04E+014	0.0	1.5286E+04
Mei et al.	1.37E+13	0.24	1.444E+04

Units are cm^3 mol s cal K, $k = A\ T^n\ exp(-E_a/RT)$

Finally, according to Bertolino et al. [44], hydrogen ignition and speciation are predominantly influenced by third-body efficiencies of the diluents under highly-diluted conditions. A combination of global sensitivity analysis and heuristic optimization methods in [44] suggested that third-body efficiencies for H_2O in impactful fall-off reactions such as (R17) $H_2O_2 + M \rightleftharpoons 2\ OH + M$ with $\alpha_{H2O/X} = 16.15$ and (R10) $H + O_2 + M \rightleftharpoons HO_2 + M$ with $\alpha_{H2O/X} = 14.75$. These values were integrated into the Klippensteinet al. kinetic mechanism in order to observe any potential impact in the ignition delay prediction because while H_2O third-body efficiencies remain largely unchanged for (R10) at 16.75 compared to 16, it varies by a factor of two for (R17). However, the observed effect does not exceed 1%.

Conclusions

This study aimed at measuring ignition delays for ultra-lean $H_2/O_2/N_2$ mixtures with equivalence ratios ranging ϕ = 0.2 – 0.5, under experimental conditions close to those observed in internal combustion engines and more specifically spark ignition engines i.e. low-to-high pressure p_C = 20 – 60 bar and low-to-intermediate temperature T_C = 900 K – 1030 K. On the other hand, the H_2/O_2 kinetic mechanism has to be chosen on the basis of internal combustion engine operating conditions as it is crucial for 0D and 3D-internal combustion engine simulations. Burke et al. kinetic mechanism is overpredicting ignition delays, by a factor of two in magnitude at maximum despite its commonly used in spark ignition engine modeling. However, recent modifications improve the accuracy of this kinetic mechanism, especially at high pressure, by the modification of the rate constant for (R17) and the addition of (R16). Other up-to-date kinetic mechanisms such as Konnov et al., Mei et al., and Sun et al. are globally in good agreement with the present work. The difference between Klippenstein et al. model and the others resides in the inclusion of the HO_2 reaction (R16). Then, the addition of this reaction into the other chemical systems was done in order to see the impact of this reaction on their respective predictions. Generally, ignition delays decrease with (R16) addition. The sensitivity analysis highlights that the inclusion of reaction (R16) in Klippenstein et al. kinetic mechanism tends to promote reactivity, countering the inhibiting effect of (R17) on model reactivity compared to Mei et al. model where the rate constant of (R17) is already fast enough.

Acknowledgment

The support of the Agence Nationale de Recherche under grant number 21-CE05-21032 (SPEEDYH ANR Project) is gratefully acknowledged.

Appendix A. Supplementary data

Supplementary data related to this article can be found in supplementary materials.

References

[1] IPCC. Climate Change 2021: The Physical Science Basis. Contribution of Working Group I to the Sixth Assessment Report of the Intergovernmental Panel on Climate Change, volume In Press. 2021.

[2] IPCC. Climate Change 2022: Mitigation of Climate Change. Contribution of Working Group III to the Sixth Assessment Report of the Intergovernmental Panel on Climate Change. 2022.

[3] IEA. Global Energy and Climate Model. 2022.

[4] IEA. Greenhouse gas emissions from energy. Annual time series of GHG emissions from energy, a major source of anthropogenic emissions. 2022.

[5] Lhuillier C, Brequigny P, Contino F, Mounaïm-Rousselle C. Experimental study on ammonia/hydrogen/air combustion in spark-ignition engine conditions. Fuel, 2019;269:117448.

[6] Verhelst S. Recent progress in the use of hydrogen as a fuel for internal combustion engines. Int J Hydrogen Energ, 2014;39:1071–1085.

[7] Unni JK, Govindappa P, Das LM. Development of hydrogen fuelled transport engine and field tests on vehicles. Int J Hydrogen Energ, 2016;42:643-651.

[8] Dimitriou P, Tsujimura T. A review of hydrogen as a compression ignition engine fuel. Int J Hydrogen Energ, 2017;42:24470.

[9] Antunes A, Mikalsen R, Roskilly T. An investigation of hydrogen-fuelled HCCI engine performance and operation. Int J Hydrogen Energ, 2008;33:5823–5828.

[10] Das LM. Hydrogen engines: A view of the past and a look into the future. Int J Hydrogen Energ, 1990;15:425.

[11] Hamzehloo A, Aleiferis P. Numerical modelling of mixture formation and combustion in DISI hydrogen engines with various injection strategies. SAE Technical Papers, 2014.

[12] Law CK, Sung CJ. Structure, aerodynamics, and geometry of premixed flamelets. Prog Energ Combust Sci, 2000;26:459.

[13] Goldsborough S Scott, Hochgreb S, Vanhove G, Wooldridge Margaret S, Curran Henry J, Sung CJ Advances in rapid compression machine studies of low and intermediate-temperature autoignition phenomena. Progress Energ Combust Sci, 2017;63:1.

[14] Pang G, Davidson D, Hanson R. Experimental study and modeling of shock tube ignition delay times for hydrogen–oxygen–argon mixtures at low temperatures. Proc Comb Inst, 2009;32:181.

[15] Hu E, Pan L, Gao Z, Lu X, Meng X. Shock tube study on ignition delay of hydrogen and evaluation of various kinetic models. Int J Hydrogen Energ, 2016:41;13261.

[16] Pan L, Zhang Y, Niu S, Tian Z. Shock tube and kinetic study of C2H6/H2/O2/Ar mixtures at elevated pressures. Int J Hydrogen Energ, 2014;39:6024.

[17] Shi Z, Zhang H, Lu H, Liu H, Yunsheng A, Meng F. Autoignition of DME/H2 mixtures in a rapid compression machine under low-to-medium temperature ranges. Fuel, 2017;194:50.

[18] Gersen S, Anikin NB, Mokhov AV, Levinsky HB. Ignition properties of methane/hydrogen mixtures in a rapid compression machine. Int J Hydrogen Energ, 2008;33:1957.

[19] Gersen S, Darmeveil H, Levinsky H. The effects of CO addition on the autoignition of H2, CH4 and CH4/H2 fuels at high pressure in an RCM. Combust Flame, 2012;159:3472.

[20] Pochet M, Dias V, Moreau B, Foucher F, Jeanmart H, Contino F. Experimental and numerical study, under LTC conditions, of ammonia ignition delay with and without hydrogen addition. Proc Combust Inst, 2018;37:621.

[21] Lee D, Hochgreb S. Hydrogen autoignition at pressures above the second explosion limit (0.6-4.0 MPa). Int J Chem Kinet, 1998;30:385.

[22] Mittal G, Sung CJ, Yetter R. Autoignition of H2/CO at elevated pressures in a rapid compression machine. Int J Chem Kinet, 2006;38:516.

[23] Mittal G, Sung CJ, Fairweather M, Tomlin A, Griffiths J, Hughes K. Significance of the HO2 + CO reaction during the combustion of CO + H2 mixtures at high pressures. Proc Comb Inst, 2007;31:419.

[24] Ó Conaire M, Curran HJ, Simmie J, Pitz W, Westbrook CK. A comprehensive modeling study of hydrogen oxidation. Int J Chem Kinet, 2004;36:603.

[25] Das A, Sung CJ, Zhang Y, Mittal G. Ignition delay study of moist hydrogen/oxidizer mixtures using a rapid compression machine. Int J Hydrogen Energ, 2012;37:6901.

[26] Kéromnès A, Metcalfe W, Heufer A, Donohoe N, Das A, Sung CJ, Herzler J, Naumann C, Griebel P, Mathieu O, Krejci M, Petersen E, Pitz W, Curran HJ. An experimental and detailed chemical kinetic modeling study of hydrogen and syngas mixture oxidation at elevated pressures. Combust Flame, 2013;160:995.

[27] Burke MP, Chaos M, Ju Y, Dryer FL, Klippenstein SJ. Comprehensive H_2/O_2 Kinetic Model for High-Pressure Combustion. Int J Chem Kinet, 2012;44 :7.

[28] Li J, Zhao Z, Kazakov A, Dryer FL. An Updated Comprehensive Kinetic Model of Hydrogen Combustion. Int J Chem Kinet, 2004;36.

[29] Manzoor UM, Yosri MR, Talei M, Poursadegh F. Normal and knocking combustion of hydrogen: A numerical study. Fuel, 2023;344.

[30] Liu X, Aljabri H, Silva M, AlRamadan AS, Houidi MB, Cenker E, Im HG. Hydrogen pre-chamber combustion at lean-burn conditions on a heavy-duty diesel engine: A computational study. Fuel, 2023;335.

[31] Babayev R, Im HG, Andersson A, Johansson B. Hydrogen double compression expansion engine H2DCEE: A sustainable internal combustion engine with 60%+ brake thermal efficiency potential at 45 bar BMEP.Ener Conver Manage, 2022;264.

[32] Burke MP, Klippenstein SJ, Harding LB. A quantitative explanation for the apparent anomalous temperature dependence of $OH + HO_2 = H_2O + O_2$ through multi-scale modeling. Proc Comb Inst, 2013;34.

[33] Klippenstein SJ, Sivaramakrishnan R, Burke U, Somers KP, Curran HJ, Cai L, Pitsch H, Pelucchi M, Faravelli T, Glarborg P. $HO_2 + HO_2$: High level theory and the role of singlet channels. Combust Flame, 2022;243.

[34] Konnov A. Yet another kinetic mechanism for hydrogen combustion. Combust Flame, 2019;203:14.

[35] Mei B, Zhang J, Shi X, Xi Z, Li Y. Enhancement of ammonia combustion with partial fuel cracking strategy: Laminar flame propagation and kinetic modeling investigation of NH3/H2/N2/air mixtures up to 10 atm. Combust Flame, 2021;231:111472.

[36] Sun W, Zhao Q, Curran HJ, Fuquan D, Zhao N, Zheng H, Kang S, Zhou X, Kang Y, Deng Y, Zhang Y. Further insights into the core mechanism of H2/CO/NOx reaction system. Combust Flame, 2022;245:112308.

[37] Bourgeois N, Goldsborough S, Jeanmart H, Contino F. CFD simulations of rapid compression machines using detailed chemistry: Evaluation of the 'crevice containment' concept. Combust Flame, 2018;189:22.

[38] Moffat RJ. Describing the uncertainties in experimental results. Experimental Thermal and Fluid Science, 1988.

[39] Baigmohammadi M, Patel V, Martinez S, Panigrahy S, Ramalingam A, Burke U. & Curran H.J. A comprehensive experimental and simulation study of ignition delay time characteristics of single fuel C1–C2 hydrocarbons over a wide range of temperatures, pressures, equivalence ratios, and dilutions. Energy & Fuels, 2020;34(3),3755-3771.

[40] Kee RJ, Rupley FM, Miller JA. Chemkin-II-A Fortran chemical kinetics package for the analysis of gas-phase chemical kinetics. J Chem Inf Model 1989;53:1689-99.

[41] Hashemi H, Christensen JM, Gersen S, Glarborg P. Hydrogen oxidation at high pressure and intermediate temperatures: Experiments and kinetic modeling. Proc Comb. Inst, 2015;35.

[42] Shrestha KP, Seidel L, Zeuch T, Mauss F. Detailed Kinetic Mechanism for the Oxidation of Ammonia Including the Formation and Reduction of Nitrogen Oxides. Energy Fuels, 2018;32.

[43] Sánchez A, Williams F. Recent advances in understanding of flammability characteristics of hydrogen. Prog Energ Comb Sci, 2014;41:01.

[44] Bertolino A, Frassoldati A, Cuoci A, Parente A. Estimation of third body efficiencies from experimental data: Application to hydrogen combustion. Int J Hydrogen Energ, 2023.